Science Advances
AAAS

Supplementary Materials for

Oxysterol misbalance critically contributes to Wilson disease pathogenesis

Som Dev *et al.*

Corresponding author: Svetlana Lutsenko, lutsenko@jhmi.edu; James P. Hamilton, jpahamilton@jhmi.edu

Sci. Adv. **8**, eadc9022 (2022)
DOI: 10.1126/sciadv.adc9022

This PDF file includes:

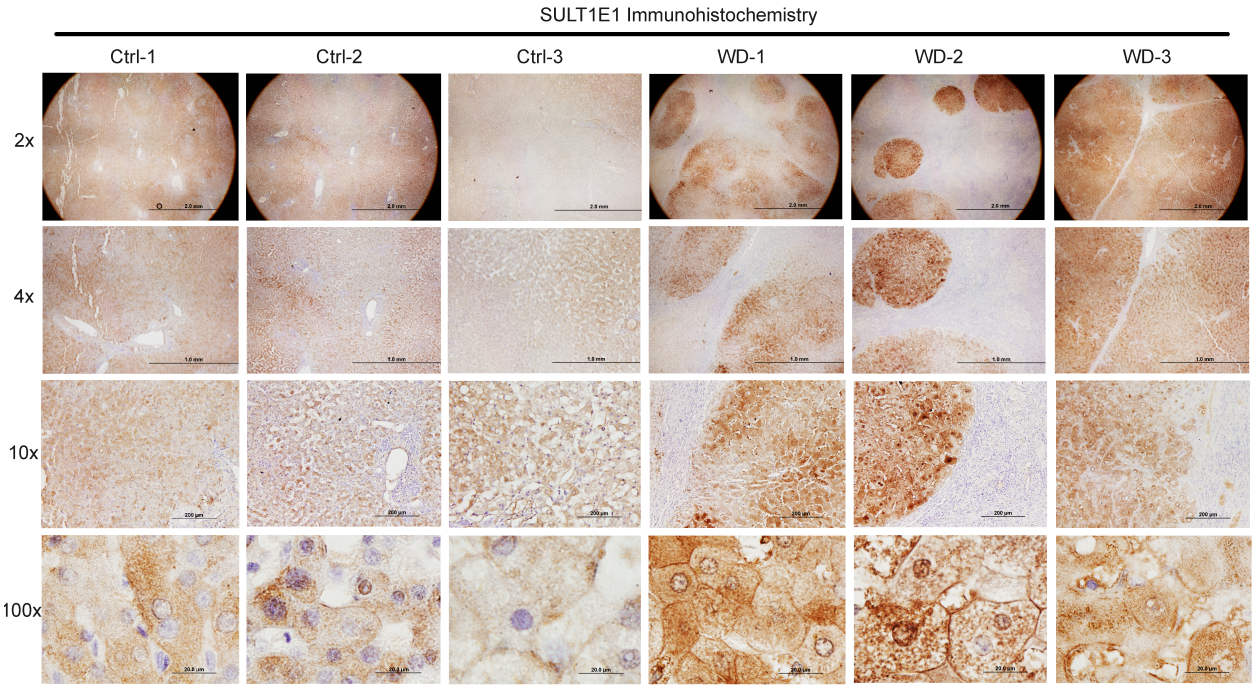

Fig. S1. SULT1E1 expression is induced in WD. Immunohistochemistry of SULT1E1 in the WD patient liver sections shows strong SULT1E1 signal in hepatocytes (right side panel) as compared to healthy controls (left side panel) as indicated by different magnifications. Scale bar-2 mm, 1 mm, 200 μm & 20 μm, n=3/group respectively.

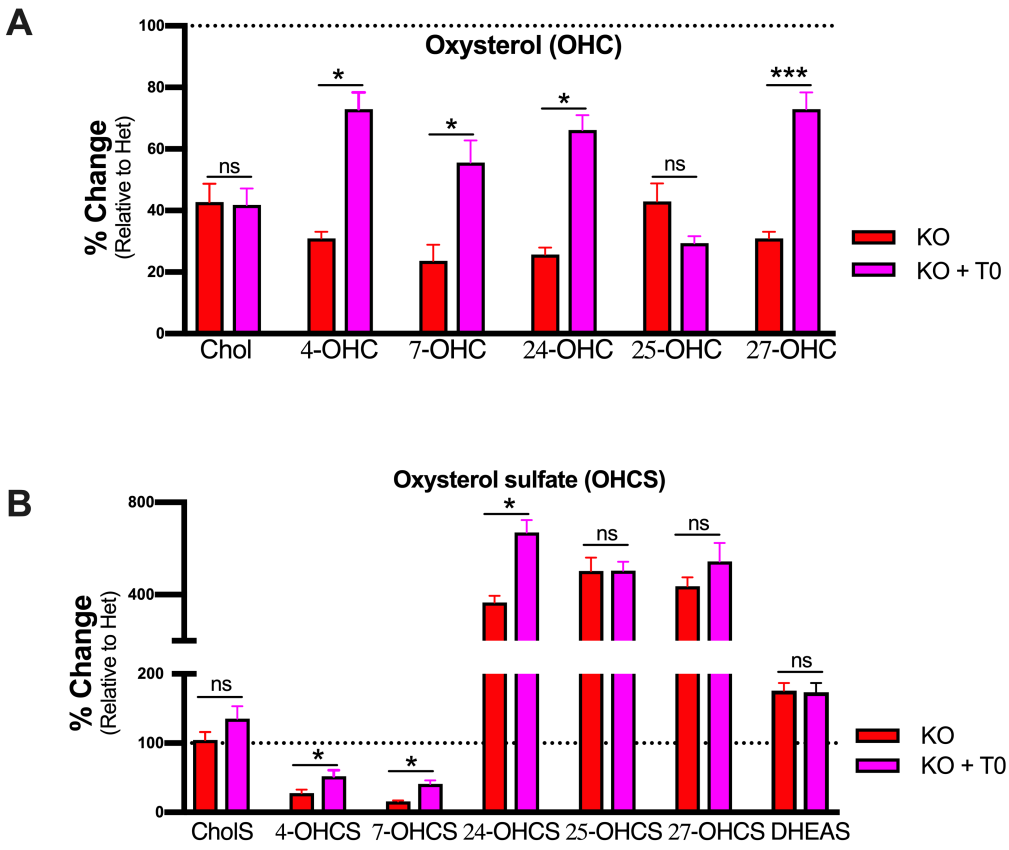

Fig. S2. LXR agonist (T0901317) primarily regulates oxysterol synthesis. (**A**) Liver oxysterols were significantly reduced in KO mice relative to Het (100%). Treatment with LXR agonist significantly elevated OHC (4-OHC, 7-OHC, 24-OHC, 27-OHC) in KO mice as compared to untreated KO. (**B**) Oxysterol sulfates (24-OHCS, 25-OHCS, 27-OHCS, DHEAS) were significantly elevated in the KO liver relative to Het (100%). Treatment with LXR agonist does not affect 25-OHCS, 27-OHCS, DHEAS, and CholS level in KO mice as compared to untreated KO. However, it increases 4-OHCS, 7-OHCS, 24-OHCS level in KO mice. Values represent mean ± SD. *P<0.05, **P<0.01, ***P<0.001, n=6 male mice/group. Red color denotes KO and magenta KO + T0, respectively. Abbreviations: Chol-Cholesterol; 4-OHC-4-Hydroxycholesterol; 7-OHC-7-Hydroxycholesterol; 24-OHC-24-Hydroxycholesterol, 25-OHC-25-Hydroxycholesterol; 4-OHCS-4-Hydroxychole-sterol-3-sulfate; 7-OHCS-7-Hydroxycholesterol-3-sulfate, 24-OHCS-24-Hydroxy-cholesterol-3-sulfate; 25-OHCS-25-Hydroxycholesterol-3-sulfate; 27-OHCS-27-Hydroxycholesterol-3-sulfate; DHEAS-Dehydroepiandrosterone sulfate; T0, T0901317; ns, non-significant.

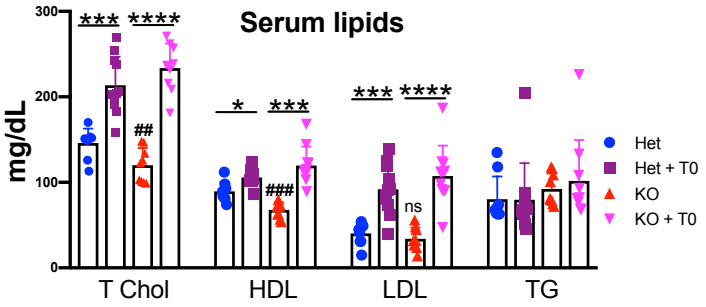

Fig. S3. LXR agonist (T0901317) upregulates lipid metabolism. Serum lipids (Total Chol, HDL, LDL) were reduced in untreated KO female mice and were elevated in the treated female mice (both Het and KO), whereas TG levels remain unchanged. Statistical comparisons were made using ANOVA with Tukey's post-hoc test. Values represent mean ± SD. *$p < 0.05$, **$p < 0.01$, ***$p < 0.001$, ****$p < 0.0001$ between untreated and treated mice of the same genotype; $^{\#}p < 0.05$, $^{\#\#}p < 0.01$, $^{\#\#\#}p < 0.001$ between untreated Het vs. KO mice, n=8-11 mice per group. Blue color denotes Het, purple Het + T0, red KO, and magenta KO + T0, respectively. Abbreviations: T0, T0901317; ns, non-significant.

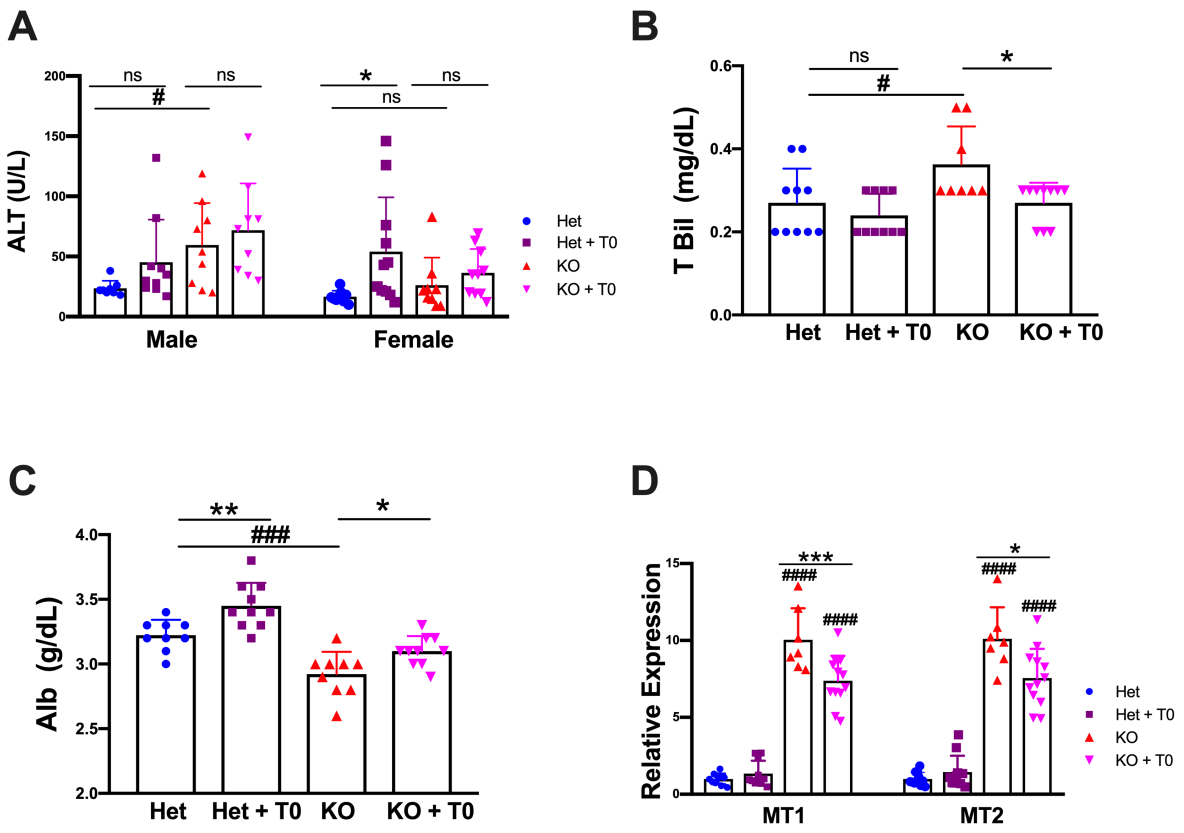

Fig. S4. LXR agonist partially improves liver function. (**A**) T0901317 treatment does not affect serum ALT levels in male and female KO mice. (**B-C**) LXR agonist reduces total serum bilirubin and increases albumin in drug-treated female KO mice. (**D**) Endogenous Cu chelators metallothioneins (MT1 and MT2) mRNA levels were remained significantly up-regulated in untreated KO and drug treated KO mice liver, and drug treatment reduces metallothionein level partly. Values represent mean ± SD. *$p < 0.05$, **$p < 0.01$, ***$p < 0.001$ between untreated and treated mice of the same genotype; $^{\#}p < 0.05$, $^{\#\#}p < 0.01$, $^{\#\#\#}p < 0.001$, $^{\#\#\#\#}p < 0.0001$ between untreated Het vs. KO mice, n=8-11 mice per group. The blue color symbol denotes Het, purple Het + T0, red KO, and magenta KO + T0, respectively. Abbreviations: T0, T0901317; ns, non-significant.

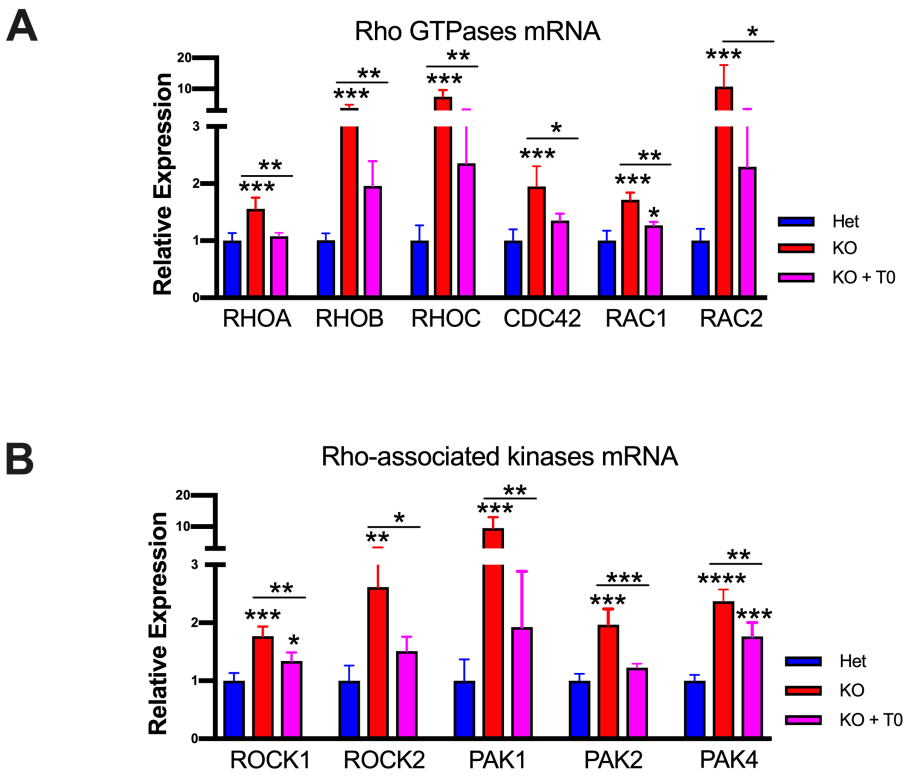

Fig. S5. LXR agonist reduces Rho GTPase signaling in *Atp7b*$^{-/-}$ mice liver. (**A-B**) Rho GTPases (RhoA-C, CDC42, RAC1, and RAC2) and Rho-associated kinases (ROCK1, ROCK2, PAK1, PAK2, PAK4) mRNA expression were significantly induced in KO mice liver as compared to Het. LXR agonist significantly reduced Rho GTPases and Rho-associated kinases mRNA level in KO mice compared to untreated KO. Values represent mean ± SD. *P<0.05, **P<0.01, ***P<0.001, ****P<0.0001, n=4 male mice/group. Blue color denotes Het, red KO and magenta KO + T0, respectively. Abbreviations: T0, T0901317; ns, non-significant.

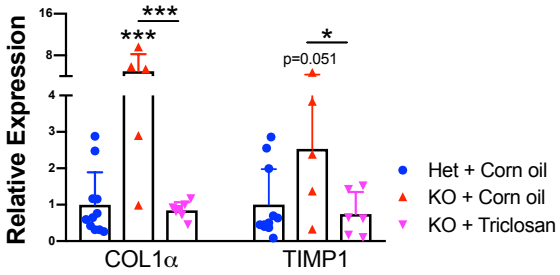

Fig. S6. Sult1e1 inhibition reduces fibrotic genes expression in *Atp7b*$^{-/-}$ mice. Fibrosis markers (Col1α and Timp1) expression is significantly induced in KO male mice liver at 12-wk, and triclosan treatment reduces their level significantly. Values represent mean ± SD. *p < 0.05, **p < 0.01, ***p < 0.001, n=5-10 mice per group. Blue color symbol denotes Het + corn oil, red KO + corn oil and magenta KO + triclosan, respectively.

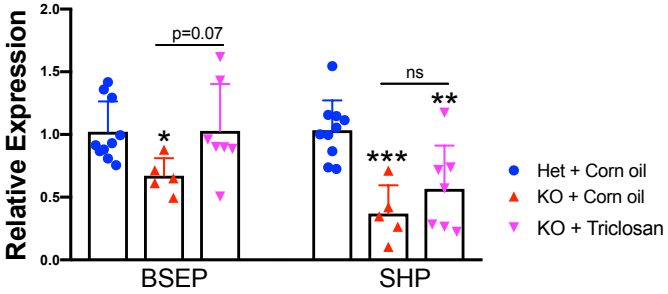

Fig. S7. Sult1e1 inhibition does not restore FXR target genes expression. FXR targets (BSEP and SHP) expression is significantly reduced in KO male mice liver at 12-wk, and triclosan treatment does not improve their level significantly. Values represent mean ± SD. *p < 0.05, **p < 0.01, ***p < 0.001, n=5-10 mice per group. Blue color symbol denotes Het + corn oil, red KO + corn oil and magenta KO + triclosan, respectively. Abbreviations: ns, non-significant.

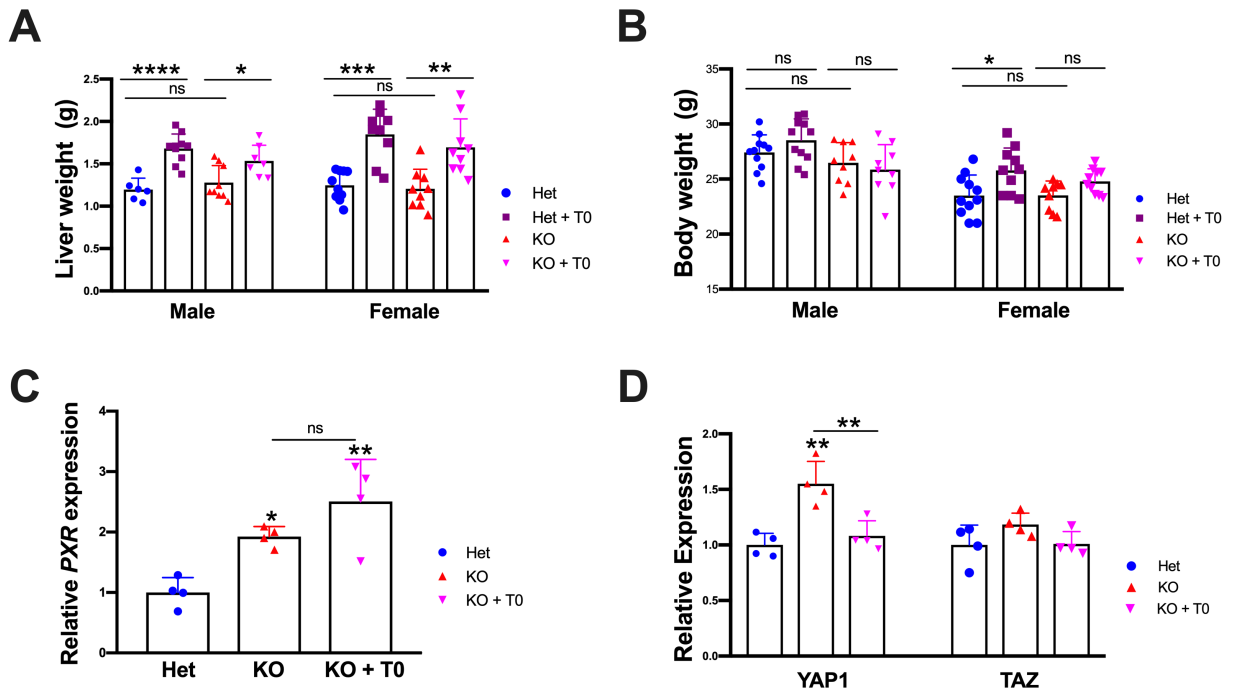

Fig. S8. LXR agonist induces liver enlargement in *Atp7b*$^{-/-}$ mice without large impact on body weight and PXR/YAP1 signaling. (**A**) LXR agonist-induced liver enlargement in male (left panel) and female (right panel) mice irrespective of genotype. (**B**) No significant change in body weight analysis was observed in males while a small increase in body weight observed in female Het mice in response to drug treatment. Statistical comparisons were made using ANOVA with Tukey's post-hoc test. Values represent mean ± SD. *p < 0.05, **p < 0.01, ***p < 0.001, ****p < 0.0001 between untreated and treated mice of the same genotype, n=8-11 mice per group, (**C-D**) Significant increase in the PXR, YAP1, and TAZ transcripts level in the KO male mice, and LXR agonist did not increase their level further in *Atp7b*$^{-/-}$ mice (KOD vs. KO). The blue color symbol denotes Het, purple Het + T0, red KO, and magenta KO + T0, respectively. Values represent mean ± SD. *p < 0.05, **p < 0.01, n=4 mice per group, Abbreviations: T0, T0901317; ns, non-significant.

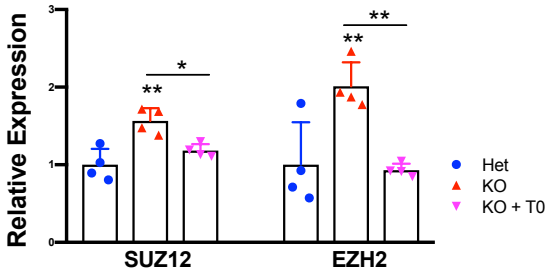

Fig. S9. Transcriptomic analysis in *Atp7b*$^{-/-}$ mice. Significant increase in the SUZ12 and EZH2 expression level in the KO male mice liver, and LXR agonist treatment reduces their level significantly in KO mice. Values represent mean ± SD. *p < 0.05, **p < 0.01, n=4 mice per group. Blue color denotes Het, red KO, and magenta KO + T0, respectively. Abbreviations: T0, T0901317.

Table S1. Expression of NRF2 target genes in *Atp7b*$^{-/-}$ mice liver

NRF2 regulated system	Gene symbol	Gene name	Het (TPM) (n=4)	KO (TPM) (n=4)	KO vs Het p Val
GSH-based system	Gpx4	Glutathione peroxidase 4	301.3	533.8	0.045
	Gsr1	Glutathione reductase	45.36	101.9	0.003
	Gss	Glutathione synthetase	44.45	116.1	0.0008
	Slc7a11	Cystine/glutamate transporter	0.13	0.60	0.04
	Gpx2	Glutathione peroxidase 2	0	19.0	0.22
TXN-based system	Txn1	Thioredoxin	252.1	481.3	0.002
	Txnrd1	Thioredoxin reductase 1	52.0	117.8	0.006
	Txnip	Thioredoxin interacting protein	41.61	141.6	0.01
	Srxn1	Sulfiredoxin 1	16.03	89.27	0.001
	Prdx1	Peroxiredoxin 1	2.95	5.48	0.003
ROS & detoxification	Gstm1	Glutathione S-transferase mu 1	1264	2496	0.007
	Ephx1	Epoxide hydrolase 1	311.2	1219.4	0.0007
	Sult1a1	Sulfotansferase 1A1	204.6	430.3	0.001
	Abcc2	ATP-binding cassette, sub-family C 2	100.6	196	0.001
	Gsta4	Glutathione S-transferase alpha 4	90.87	180.6	0.034
	Gstm3	Glutathione S-transferase mu 3	63.12	850.1	0.02
	Gstm2	Glutathione S-transferase mu 2	59.8	299.6	0.023
	Gsta1	Glutathione S-transferase alpha 1	5.27	223.9	0.003
	Gsta2	Glutathione S-transferase alpha 2	36.82	129.0	7E-05
	Sod3	Superoxide dismutase 3, extracellular	13.19	38.94	0.005
	Akr1b8	Alpha keto reductase family 1, B8	5.88	20.88	0.05
	Nqo1	NAD(P)H quinone dehydrogenase 1	4.33	44.57	0.03
	Akr1b3	Alpha keto reductase family 1, B3	1.85	4.87	0.01
	Adh7	Alcohol dehydrogenase class	1.17	4.05	0.0001
	Abcc1	ATP-binding cassette, sub-family C 1	0.75	3.05	0.02
	Sult1e1	Sulfotansferase 1E1	0.26	148.9	0.0006
	Mgst2	Microsomal glutathione S-transferase	0	82.88	0.003
NADPH regeneration	Idh1	Isocitrate dehydrogenase 1, NADP(+)	321.5	512.9	0.005
	Me1	Malic enzyme 1, NADP(+) cytosolic	58.24	83.85	0.08
	Pgd	Phosphogluconate dehydrogenase	8.91	44.4	0.006
	G6pd	Glucose-6-phosphate dehydrogenase	2.97	11.96	0.03
Heme & Fe system	Ft-L	Ferritin-L	5582.2	8438.8	0.005
	Ft-H	Ferritin-H	869.2	1655.6	0.009
	BlvrB	Biliverdin reductase B	122.3	366.9	0.008
	Hmox1	Heme oxygenase 1	32.96	123.2	0.02
Transcription (TF)	Nrf2	Nuclear factor, erythroid derived 2, like 2	22.47	74.67	0.02
	Maf	avian musculoaponeurotic fibrosarcoma oncogene homolog	11.59	21.34	0.02
	MafG	v-maf musculoaponeurotic fibrosarcoma oncogene homolog G	10.20	23.01	0.0004
	MafK	v-maf musculoaponeurotic fibrosarcoma oncogene homolog K	4.91	17.73	0.0001

TPM- Transcript per million

Table S2. Top upstream regulators in *Atp7b*$^{-/-}$ mice liver (IPA)

S. NO.	Name	Molecule type	z-score	p-value	Targets
1	IFNG	Cytokine	9.28	$6.75x10^{-45}$	867
2	TGFβ1	Growth factor	2.86	$1.55x10^{-35}$	1227
3	NR1H3 (LXRα)	Ligand-dependent nuclear receptor	-0.8	$1.06x10^{-33}$	921
4	TP53	Transcription regulator	0.95	$1.02x10^{-30}$	969

IFNG- Interferon γ; TGFβ1-Transforming growth factor β1; NR1H3-Nuclear Receptor Subfamily 1 Group H Member 3; TP53-Tumor protein P53; IPA-Ingenuity pathway analysis

Table S3. Sterol analysis in the *Atp7b*$^{-/-}$ mice with age (LC-MS/MS)

Sterols (pg/mg of tissue)	**12-wk Het vs KO** (*p value*)	**Change** (%)	**20-wk Het vs KO** (*p value*)	**Change** (%)
Oxysterol				
Chol	4141 vs 3264 (*p=0.11*)	21.1 %	3568 vs 1527 (*p=0.001*)	57.2 % ↓
4-OHC	523 vs 249 (*p=0.0003*)	52.3 % ↓	415 vs 128.6 (*p=0.0002*)	69 % ↓
7-OHC	838 vs 319 (*p=<0.0001*)	61.9 % ↓	666.7 vs 158 (*p=<0.0001*)	76.3 % ↓
24-OHC	712 vs 201 (*p=<0.0001*)	71.7 % ↓	887.1 vs 227.7 (*p=<0.0001*)	74.4 % ↓
25-OHC	1115 vs 494.2 (*p=<0.0001*)	55.6 % ↓	566 vs 243.3 (*p=<0.0001*)	57 % ↓
27-OHC	1874 vs 859.2 (*p=<0.0001*)	54.1 % ↓	678.3 vs 914.3 (*p=0.32*)	34.8 %
Oxysterol sulfate				
CholS	752.2 vs 1283 (*p=0.01*)	70 % ↑	602 vs 630 (*p=0.99*)	4.6 %
4-OHCS	335.9 vs 261.2 *(0.06)*	22.2 % ↓	341.7 vs 96.0 (*p=<0.0001*)	71.8 % ↓
7-OHCS	273 vs 99 (*p=<0.0001*)	63.7 % ↓	177.8 vs 28.0 (*p=<0.0001*)	84 % ↓
24-OHCS	293 vs 836.2 (*p=<0.0001*)	185 % ↑	153.2 vs 561.1 (*p=<0.0001*)	266 % ↑
25-OHCS	254.5 vs 1059 (*p=<0.0001*)	316 % ↑	143.6 vs 721.5 (*p=<0.0001*)	402 % ↑
27-OHCS	649.8 vs 1608 (*p=<0.0001*)	147 % ↑	522.7 vs 2280 (*p=0.0002*)	336 % ↑
DHEAS	503.3 vs 1188 (*p=<0.0001*)	136 % ↑	396.2 vs 694.4 (*p=0.0002*)	75 % ↑

n=6 male mice/group

Chol-Cholesterol; 4-OHC-4-Hydroxycholesterol; 7-OHC-7-Hydroxycholesterol; 24-OHC-24-Hydroxycholesterol; 27-OHC-27-Hydroxycholesterol; 4-OHCS-4-Hydroxycholesterol-3-sulfate; 7-OHCS-7-Hydroxycholesterol-3-sulfate; 24-OHCS-24-Hydroxycholesterol-3-sulfate; 27-OHCS-27-Hydroxycholesterol-3-sulfate; DHEA-Dehydroepiandrosterone sulfate

Table S4. List of antibodies used in the study

Antibodies	Company	Cat No	Dilution
p38α/β	Santa Cruz	sc-7972	1:1000 (WB)
ERK1/2	Cell Signaling	4695	1:2000 (WB)
JNK	Cell Signaling	9252	1:1000 (WB)
SMAD2	Cell Signaling	5339	1:1000 (WB)
Anti-Rabbit HRP	Cell Signaling	7074	1:5,000 (WB)
Anti-Mouse HRP	Cell Signaling	7076	1:5,000 (WB)
GAPDH-HRP	Sigma	G9295	1:10,000 (WB)
NRF2	Cell Signaling	12721	1:1,000 (WB), 1:100 (IF)
Lamin A	Abcam	Ab26300	1:1000 (WB)
F4/80	Abcam	ab90247	1:100 (IF)
Desmin	Abcam	ab32362	1:50 (IF)
TGFβRII	Abcam	sc-17792	1:100 (IF)
DARat Alexa fluor 488	Invitrogen	A21208	1:500 (IF)
DARb Alexa fluor 647	Invitrogen	A31573	1:500 (IF)
DARb Alexa fluor 488	Invitrogen	A21206	1:500 (IF)
DAM Alexa fluor 647	Invitrogen	A31571	1:500 (IF)
GARat Alexa fluor 488	Invitrogen	A11077	1:500 (IF)
SULT1E1	Santa Cruz	sc-376009	1:250(m); 1:100(h) (IHC)
TGFβ1	Santa Cruz	sc-130348	1:250 (IHC)
Biotinylated Anti mouse IgG	Vector Lab	BA-9200	1:1000 (IHC)

DARat- Donkey Anti Rat; DARb-Donkey Anti Rabbit; DAM-Donkey Anti Mouse; GARat-Goat Anti Rat
WB-Western Blotting; IF-Immunofluorescence; IHC-Immunohistochemistry

Table S5. List of primers (Mus musculus) used for qRT-PCR

S. No	Primer	Sequence
1	ATP7B	5'-TTCTTGCGTCAAGTCCATTG-3' 5'-CCTCAAAGCCATATCCTCA-3
2	MT1	5'-CACTTGCACCAGCTCCTG-3' 5'-GAAGACGCTGGGTTGGTC-3'
3	MT2	5'-GCAAACAATGCAAATGTACTTCC-3' 5'-CTATTTACACAGATGTGGGGACC-3'
4	SULT1E1	5'-CTCGCTGACATCATCCTCGC-3' 5'-GCGTTTTGTTGCCGTAGCA-3'
5	COX2	5'-TGAGCAACTATTCCAAACCAG-3' 5'-GCACGTAGTCTTCGATCACTATC-3'
6	TNFα	5'-CTGTGAAGGGAATGGGTGTT-3' 5'-GGTCACTGTCCCAGCATCTT-3'
7	iNOS	5'-CCTTGTTCAGCTACGCCTTC-3' 5'-AAGGCCAAACACAGCATACC-3'
8	IL-6	5'-TAGTCCTTCCTACCCCAATTTCC-3' 5'-TTGGTCCTTAGCCACTCCTTC-3'
9	COL1A1	5'-GAGCGGAGAGTACTGGATCG-3' 5'-TACTCGAACGGAATCCATC-3'
10	TIMP1	5'-CGAGACCACCTTATACCAGCG-3' 5'-ATGACTGGGGTGTAGGCGTA-3'
11	IL-1β	5'-GAAATGCCACCTTTTGACAGTG-3' 5'-TGGATGCTCTCATCAGGACAG-3'
12	CD24A	5'-GAAAGGGGGCTTGGTTCTAC-3' 5'-TCCTTCTTCCCAGGAAGGTT-3'
13	FASN	5'-CTGCCTTCGGTTCAGTCTC-3' 5'-AGTCTCACTGGAAGAGCTGTG-3'
14	SCD1	5'-TTCTTGCGATACACTCTGGTGC-3' 5'-CGGGATTGAATGTTCTTGTCGT-3'
15	SHP	5'-TATGCGTACCTGAAGGGCAC-3' 5'-CCAGGGCTCCAAGACTTCAC-3'
16	BSEP	5'-AGGTTGTGGGTAATCACTGGG-3' 5'-TCAAACCATCCGATTTCCATTCT-3'
17	ABCA1	5'-AAAACCGCAGACATCCTTCAG-3' 5'-CATACCGAAACTCGTTCACCC-3'
18	ABCG5	5'-ACCCTTGTGTCTGACCCTTG-3' 5'-CACAATGTCCAAGCACCACAT-3'
19	ABCG8	5'-CAGGTGCCTTGGTTTGAGC-3' 5'-CTTAGATTTCGGATGCCCAGC-3'
20	CYP7A	5'-GCTGTGGTAGTGAGCTGTTG-3' 5'-GTTGTCCAAAGGAGGTTCACC-3'
21	RPL19	5'-CCCGTCAGCAGATCAGGAA-3' 5'-GTCACAGGCTTGCGGATGA-3'

ATP7B-ATPase Cu^{++} transporting beta polypeptide; MT-Metallothionein; SULT1E1-Sulfotransferase1E1; COX2-Cyclooxygenase-2; IL-6-Interleukin-6; TNFα-Tumor Necrosis Factor-alpha; FASN-Fatty Acid Synthase; SCD1-Stearoyl CoA desaturase 1; IL-1β-Interleukin-1beta; INOS-Inducible Nitric Oxide Synthase; COL1α-Collagen 1alpha; TIMP1-Tissue Inhibitor of Metalloproteinase1; CD24A-Cluster of differentiation 24; SHP- Small heterodimer partner; BSEP-Bile salt export pump; ABCG5-ATP Binding Cassette Subfamily G Member 5; ABCG8-ATP Binding Cassette Subfamily G Member 8; ABCA1-ATP-binding cassette transporter; RPL19-Ribosomal Protein L19

Table S6. Mass spectral parameters used to identify (Pseudo-MRM) and quantify (MRM) each sterol derivative from liver tissue samples

S. NO.	Analyte	Pseudo MRM	MRM	CE	Retention time
1	Cholesterol	369.40<369.40	369.40<161.50	10,40	8.02
2	4-Hydroxycholesterol	385.40<385.40	385.40<109.41	12,40	7.73
3	7-Hydroxycholesterol	385.41<385.41	367.35<159.12	10,40	7.30
4	24-Hydroxycholesterol	385.42<367.42	367.40<95.03	10,40	6.95
5	25-Hydroxycholesterol	385.43<367.43	367.40<147.09	10,40	7.09
6	27-Hydroxycholesterol	385.45<367.45	385.40<81.06	10,40	6.55
7	Dihydroxycholesterol	401.40<401.40	401.40<109.41	10,40	7.62
8	25-Hydroxycholesterol-D6	391.40<391.40	391.40<147.42	10,35	6.93
9	Cholesterol-3-sulfate	465.40<465.40	465.40<97.00	10,35	7.47
10	4-Hydroxycholesterol-3-sulfate	481.11<481.11	481.11<97.00	10,35	7.14
11	7-Hydroxycholesterol-3-sulfate	481.12<481.12	481.12<97.00	10,35	7.23
12	24-Hydroxycholesterol-3-sulfate	481.13<481.13	481.13<97.00	10,35	7.10
13	25-Hydroxycholesterol-3-sulfate	481.14<481.14	481.14<97.00	10,35	6.59
14	27-Hydroxycholesterol-3-sulfate	481.15<481.15	481.15<97.00	10,35	6.89
15	Pregnenolone sulfate	395.40<395.40	395.40<96.90	10,35	6.67
16	Dehydroepiandrosterone sulfate	367.50<367.50	367.50<96.90	10,35	6.98
17	Cholic acid	407.30<407.30	407.30<407.30	10,35	5.88
18	Chenodeoxycholic acid	391.30<391.30	391.30<391.30	10,35	7.10
19	Chenodeoxycholic acid -D5	396.40<396.40	396.40<396.40	10,35	6.66
20	Cholesterol sulfate-D7	494.40<494.40	494.40<97.00	10,35	7.32

Pseudo MRM- Precursor ion *m/z* to precursor ion *m/z* transition
MRM-Precursor ion *m/z* to product ion *m/z* transition
CE- Collision Energy

Table S7. Mobile phase gradient program at constant flow at 250 ul/min

S. NO.	Time	ddH2O (0.1% FA)	MeOH (0.1% FA)
1	0.05	60	40
2	2.50	5	95
3	7.50	5	95
4	12.50	40	60
5	14.00	40	60

FA- Formic acid